



A revised parameterisation of the condensation and precipitation processes  
for use in numerical forecasting models

P R Jonas

122314

## 1. Introduction

In recent years a considerable effort has been devoted to the development of numerical models of the atmosphere for forecasting over periods of a few days ahead. In addition to the forecasting of dynamical development the models are sometimes used directly to obtain quantitative precipitation forecasts. Water vapour is frequently carried as a variable by these models and various approximations are made to derive the latent heating by condensation and the conversion from condensed water to precipitation. For example in the operational model used by the Meteorological Office (Bushby and Timpson, 1967, Benwell et al, 1971) it is assumed that no condensation occurs until saturation is obtained and that, following condensation, all of the condensed water is precipitated. In this model the precipitated water falls instantaneously to the ground subject to evaporation at lower levels. In other models similar assumptions may be made but condensation and precipitation of the liquid water occur when some threshold relative humidity, typically 80%, is reached.

While these formulations may predict rainfall accumulations which are, at least over low ground, in reasonable agreement with observations (see for example Wickham, 1974), the feedback between the condensation and dynamical processes cannot be correctly represented. With the assumptions described above there is no latent heating until high relative humidities are reached on a grid scale and this will, in most cases, be followed by precipitation. This is clearly unrealistic; radio-sonde observations seldom yield relative humidities of 100% through very deep layers even in conditions of widespread continuous rain or there may be shallow layers of cloud in deep layers of low mean relative humidity. The unrealistically low rates of rainfall obtained during the early stages of Meteorological Office numerical forecasts are due, in part, to the time taken for the dynamical processes to increase the relative humidity from observed values in regions of precipitation to 100%. This deficiency could be removed to some extent by a reduction in the threshold relative



humidity for condensation; however, latent heat released at low mean relative humidities through the formation of shallow non precipitating cloud and cooling by subsequent evaporation of this cloud would not be treated by this approximation. The possible dynamical effects of the condensation and evaporation of small amounts of water are quite large; at 850 mb the condensation of 1% of the saturated mixing ratio will release  $10^2 \text{ J kg}^{-1}$  of energy, equivalent to a temperature increase of 0.1 C or to a velocity increase of  $14 \text{ ms}^{-1}$ . Although latent heat is normally realised as potential, rather than kinetic, energy it is clear that latent heating is an important energy source, or sink, and should be treated accurately in numerical models.

In this note a scheme is described for parameterising the condensation and precipitation processes in numerical models. Note is taken of the variability of relative humidity on a sub grid scale both in the vertical and in the horizontal and this gives rise to condensation at low mean relative humidities. Precipitation results from a conversion from cloud to precipitable water which is assumed to reduce the water mixing ratio in the clouds, which is generally larger than the grid mean liquid water mixing ratio, to some threshold value. If a steady state approximation is assumed it is possible to diagnose the rainfall rate from an initial distribution of relative humidity: such a scheme could be of use when assessing the accuracy of the relative humidity fields used for numerical forecasts. The sub grid scale variability of relative humidity which is assumed in the derivation of the parameterisation is shown to be consistent with the reported upper level relative humidity for occasions when precipitation is observed.

## 2. The parameterisation of condensation

It is a basic assumption of the parameterisation scheme that within a volume represented by a grid point in a numerical model the processes of condensation and evaporation act to distribute water between the liquid and vapour phases in proportions which depend only on the mean relative humidity within the volume. Latent heat is released or absorbed in this process but precipitation removes only liquid water with no change of temperature. We assume that as a result of dynamical



processes, or of processes such as those occurring at the surface of the earth, which result in the change of temperature and mixing ratio at a grid point the balance between the vapour and liquid phases is upset. We can then calculate the latent heating and the resultant balance.

Denoting the liquid water mixing ratio by  $l$  (although the term liquid is used this is taken to include the solid phase at low temperature, the latent heat referring to the latent heat of sublimation) and the vapour mixing ratio by  $r$  we can express the assumption above as:

$$\frac{l}{l+r} = \xi \left( \frac{l+r}{r_s(T)} \right) \quad (1)$$

where  $r_s(T)$  is the saturated mixing ratio at temperature  $T$  and the function  $\xi$  is a prescribed function of the total relative humidity. Considering condensation from an initial state represented by the value  $l_0$ ,  $r_0$  and  $T_0$  the equation for the conservation of heat gives:

$$T - T_0 = \frac{L}{c_p} (l_0 + r_0) \left\{ \xi \left( \frac{l_0 + r_0}{r_s(T)} \right) - \frac{l_0}{l_0 + r_0} \right\} \quad (2)$$

since  $l_0 + r_0 = l + r$  and where  $c_p$  and  $L$  are the specific heat of air at constant pressure and the latent heat of condensation, or sublimation, of water. The Clausius-Clapyron equation can be written in the form

$$r_s(T) - r_s(T_0) = \frac{\epsilon L}{R T_0^2} r_s(T_0) (T - T_0) \quad (3)$$

where  $\epsilon$  is the ratio of the molecular weights of water vapour and dry air and  $R$  is the universal gas constant. We can write:

$$\xi \left( \frac{l_0 + r_0}{r_s(T)} \right) = \xi \left( \frac{l_0 + r_0}{r_s(T_0)} \right) + \frac{\partial \xi}{\partial r_s} \{ r_s(T) - r_s(T_0) \} \quad (4)$$

Substituting (4) and (3) into (2) and denoting  $\partial \xi / \partial r_s$  by  $-\beta$  we obtain, after rearrangement:



$$T - T_0 = L (l_0 + r_0) \left\{ \xi \left( \frac{l_0 + r_0}{r_s(T_0)} \right) - \frac{l_0}{(l_0 + r_0)} \right\} / \left\{ c_p + \frac{\beta \epsilon L^2}{R T_0^2} (l_0 + r_0) r_s(T_0) \right\} \quad (5)$$

It should be noted that if, in this expression for the heating due to condensation, we make the assumption that all of the water in excess of that required to reach saturation is condensed, that is  $\xi((l_0 + r_0)/r_s(T_0)) = (l_0 + r_0 - r_s(T_0))/(l_0 + r_0)$  and that precipitation removes all of the condensed water so that  $l_0 \equiv 0$  then we have:

$$T - T_0 = L \{ r_0 - r_s(T_0) \} / \left\{ c_p + \frac{\epsilon L^2}{R T_0^2} r_s(T_0) \right\} \quad (5a)$$

This is identical with the expression derived by Benwell et al (1971, p 34) for this approximation. We can calculate the latent heating from (5) provided that the form of  $\xi$  is known.

In order to obtain a form for  $\xi$  we assume that within the volume represented by a grid point the total relative humidity  $(l+r)/r_s(T)$  is distributed with some mean value  $\bar{H}$  such that:

$$\int_0^{\infty} H f(H) dH = \bar{H} \quad (6)$$

where  $f(H)dH$  represents the fraction of the volume within which the humidity lies in the range  $H$  to  $H + dH$ . In regions where  $H < 1$  the liquid water mixing ratio is zero while in regions where  $H \geq 1$  the vapour mixing ratio is equal to the mean saturated mixing ratio. The mean liquid mixing ratio will then be given by:

$$l = r_s \int_{1.0}^{\infty} (H - 1.0) f(H) dH \quad (7)$$

so that:

$$\xi \left( \frac{l+r}{r_s(T)} \right) = \frac{l}{l+r} = \frac{\int_{1.0}^{\infty} (H - 1.0) f(H) dH}{\int_0^{\infty} H f(H) dH} \quad (8)$$



It was estimated from inspection of radio-sonde ascents and from the observed horizontal variations of relative humidity that the total relative humidity could be assumed to be distributed normally about  $\bar{H}$  with a standard deviation which decreased as  $\bar{H}$  increased. The normal distributions were truncated at zero relative humidity. A more detailed justification for this assumption cannot be given but the results obtained with the parameterisation scheme show that this assumption is not too unrealistic. The variation of the amount of water condensed with the total relative humidity obtained using (8) is shown in fig 1(a). Curves are plotted for constant standard deviations of total humidity of 40% and 20% and also for the case of standard deviation decreasing linearly from 40% at  $\bar{H} = 0$  to 20% for  $\bar{H} = 1.0$ . It was the latter formulation which was adopted for the parameterisation scheme used in deriving results presented later in this note. For comparison purposes a curve is also plotted in fig 1(a) showing the amount of water condensed if condensation only occurs when the mean relative humidity reaches 100%. This is equivalent to setting the standard deviation in the normal distribution to zero.

The fraction of the volume which contains cloud can readily be calculated being given by:

$$f_c = \int_{1.0}^{\infty} f(H) dH \quad (9)$$

and the mean liquid water mixing ratio in the cloud is given by:

$$L_c = r_s \int_{1.0}^{\infty} (H - 1.0) f(H) dH / \int_{1.0}^{\infty} f(H) dH \quad (10)$$

The variation of the liquid water mixing ratio in the cloud with the total relative humidity is presented in fig 1(b) for the same distribution of humidity as used for fig 1(a). It can be seen that quite large values can be obtained for the liquid water content in the cloud even if the mean relative humidity is quite low. The parameterisation of the condensation process enables calculations of the latent heating and of the cloud water mixing ratio to be obtained. It is the latter which is important in the determination of the precipitation from the cloud.



### 3. Parameterisation of the conversion from cloud water to precipitation

The formation of precipitation from cloud water depends on the water mixing ratio within the cloud and on such factors as the lifetime of the cloud and on the depth of the cloud. There are many observations of the liquid water mixing ratio in both precipitating and non precipitating layer clouds (see for example, Mason, 1971). These observations suggest that an assumption to simplify the conversion process which would not be too unrealistic, for layer clouds, would be to assume that all of the cloud water above some threshold mixing ratio is precipitated. This implies a constant liquid mixing ratio in precipitating clouds and that clouds with a lower cloud water mixing ratio do not precipitate. The threshold cloud water content decreases as the altitude increases and for the parameterisation scheme it was found convenient to assume a threshold of  $0.15 \times r_s(T)$ . This would imply a maximum cloud water mixing ratio decreasing from about  $1.1 \text{ g kg}^{-1}$  at 950 mb to about  $0.05 \text{ g kg}^{-1}$  at 350 mb. An alternative parameterisation would be to convert cloud water to precipitation at a rate dependent on the cloud water mixing ratio and possibly on the updraught. In view of the other approximations made in the parameterisation of the condensation processes, the large changes in cloud water mixing ratio which can occur during the time step of a model of atmospheric dynamics and the penalty in computation time it was felt unjustifiable to use a more detailed scheme.

The amount of water precipitated from the cloud,  $P$  will be given by

$$P = \{L_c - 0.15 \times r_s(T)\} f_c \quad (11)$$

remembering that water is only precipitation from that function  $f_c$  of the volume which contains cloud. It is assumed that this precipitation falls instantaneously from the volume and, subject to evaporation at lower levels, reaches the surface as precipitation. For the purposes of calculating a rainfall rate it is assumed that the surface precipitation resulting from dynamically produced changes in the relative humidity at a point is spread uniformly over the time step during which these changes occurred.



It has been indicated that one of the reasons for improving the parameterisation of the processes of condensation and precipitation is the inconsistency of observations of relative humidity at upper levels in occasions of precipitation and the relative humidities required to give precipitation in the numerical models. Jonas (1976) attempted to diagnose the upper level humidity averaged over a depth of 100 mb from surface observations of weather. The distribution of mean relative humidity at 850 mb was shown for occasions of surface precipitation where orographic effects could be neglected and it was seen that a very wide distribution was possible. A similar analysis has been carried out using the observations at 850 mb rather than the average values over a layer and the results are shown in fig 2. It is implied in the parameterisation scheme that precipitation falls from a volume when the mean relative humidity  $\bar{H}$  exceeds some critical value  $H_c$  and that within the volume the local relative humidity  $H_e$  is distributed about the mean value. Using the distribution of  $H_e$  for various values of  $\bar{H}$  it is possible to obtain a distribution  $P(\bar{H})d\bar{H}$  which gives:

$$\int_0^{\infty} P(\bar{H}) (P(H_e) dH_e) d\bar{H} \approx P_o(H_e) dH_e \quad (12)$$

where  $P(\bar{H})d\bar{H}$  is the probability of  $\bar{H}$  lying in the range  $\bar{H}$  to  $\bar{H}+d\bar{H}$ ,  $P(H_e)dH_e$  is the probability of  $H_e$  in the range  $H_e$  to  $H_e+dH_e$  and  $P_o(H_e)dH_e$  is the probability of an observation of relative humidity lying in the range  $H_e$  to  $H_e+dH_e$ . The assumption is made that the measured distribution of relative humidity observations at a fixed level is equivalent to the mean distribution within the volume represented by a grid point. The distribution of humidity observations on occasions of precipitation is then given by:

$$P_r(H_e) dH_e = \int_{H_c}^{\infty} P(\bar{H}) (P(H_e) dH_e) d\bar{H} \quad (13)$$

Using a distribution  $P(\bar{H})$  which gives a good approximation to (12) the distribution  $P_r(H_e)$  was calculated and this is also shown in fig 2. The agreement between the



calculated distribution at this level for occasions of rain is very good. With the observed humidity distribution at 850 mb the parameterisation scheme is consistent with rainfall on 22% of occasions. This agrees well with the observed 19% of occasions which were wet according to Jonas' classification. It can be seen therefore that the parameterisation scheme will, on average, account for the sub grid scale variations of relative humidity.

#### 4. The use of the parameterisation scheme in the 10-level model

The physical basis of the improved parameterisation schemes has been demonstrated but the ultimate test of any parameterisation is its effect when included in numerical models of the atmosphere. The schemes have therefore been tested in the operational version of the Meteorological Office 10-level model (see Benwell et al, 1971). In this model water vapour is carried as a variable at the mid points of 100 mb deep layers from 300 mb to 1000 mb. Precipitation is such as to reduce the mixing ratio to the saturated mixing ratio, after allowance for latent heating and the precipitation falls instantaneously from the layer. Evaporation may occur in lower, sub saturated layers. The main deficiencies of the rainfall forecasts, apart from those due to incorrect forecast development, are an underestimation of rainfall accumulation over 12 or 24 hr periods and very low rainfall rates in the first 6 hr of the forecast. Rainfall is not analysed and there is no indication of rainfall rate on the initial charts prepared from the data used for the numerical forecast. Two versions of the model are in use, an almost hemispheric version with a 300 km grid and a limited area model with a 100 km grid. The latter version is used to provide quantitative rainfall forecasts and it is in this limited area model that the revised parameterisation has been intensively tested, but the scheme was included in the coarse mesh version as this is used to provide background analyses and boundary changes for the limited area model.

For an operational model it is desirable to reduce computer time and the new parameterisation provides an additional variable, the liquid water mixing ratio, which should be advected in the same way as the water vapour. However the condensation and precipitation processes depend on the total relative humidity of which the liquid



water contributes at most 15%. Also, in many frontal situations the changes in relative humidity due to temperature advection are more important than those due to the advection of water. It was found that the results obtained when the advection of liquid water was neglected and when total water was the advected variable were very similar so that, in the interests of computational economy, the advection of liquid water was neglected in all of the experiments reported here.

The analyses for the operational forecasts have been obtained by methods described by Atkins (1970, 1974) and for the moisture variable relative humidity is analysed using a previous forecast as a background or first guess analysis. It is necessary to provide an initial field of liquid water mixing ratio for use in the parameterisation scheme otherwise considerable latent heating may be expected in the first step of the numerical forecast. Since there are no observations of liquid water mixing ratio, and since the radio-sonde observations provide a measure of the water vapour mixing ratio a steady state approximation is used to diagnose liquid water mixing ratio as a function of water vapour mixing ratio using the parameterisation scheme. This approximation also yields the rainfall rate as a function of the observed relative humidity.

In the numerical forecast model we treat a steady state situation producing precipitation as a cycle of convergence of moisture, condensation, fallout of precipitation and the removal of the latent heat of condensation. A difficulty then arises in the interpretation of humidity observation since in the model there are large humidity variations in the course of the cycle. We suppose that after the dynamical convergence of moisture the vapour and liquid mixing ratios are  $c_0$  and  $l_0$  and that the temperature is  $T_0$ . Condensation results in the variables being modified to  $c_I$ ,  $l_I$  and  $T_I$ . Precipitation corresponding to a reduction  $\rho$  in the liquid mixing ratio is followed by dynamical processes restoring the values  $c_0$ ,  $l_0$  and  $T_0$ . Since we neglect the advection of liquid water then  $l_I = l_0 + \rho$  and since total water is conserved during condensation  $l_0 + c_0 = l_I + c_I$  so that  $c_I = c_0 - \rho$ . Conservation of heat then enables us to calculate the temperature change during condensation  $T_I - T_0 = L\rho/c_p$ . We now suppose that we measure values



of vapour mixing ratio and temperature  $r$  and  $T$  and that the unknown liquid mixing ratio is  $L$ . As mentioned earlier the point in the cycle at which these are measured is not known so that we assume that the measurements correspond to a weighted average of conditions after convergence, before condensation and after condensation and precipitation, that is,

$$\begin{aligned} T &= AT_0 + (1-A)T_I \\ r &= Ar_0 + (1-A)r_I \\ L &= L_0 \end{aligned} \quad (14)$$

where  $0 \leq A \leq 1$ .  $A = 0$  corresponds to observations after condensation and  $A = 1$  to observations before condensation. Since  $r_I = r_0 - p$  we have from (14):

$$r = r_I + Ap \quad (15)$$

and also, since  $T_I - T_0 = Lp/c_p$ ,

$$T_I - T = A(T_I - T_0) = ALp/c_p \quad (16)$$

Substituting (16) into the Clausius-Clapyron equation yields:

$$\frac{r_s(T_I)}{r_s(T)} = 1 + \frac{AEL^2p}{Rc_p r_s(T_I)} \cdot \frac{r_s(T_I)}{T^2} \quad (17)$$

Substituting (15) into (17) and rearranging we obtain

$$\frac{r}{r_s(T)} = \left\{ \frac{r_I}{r_s(T_I)} + \frac{Ap}{r_s(T_I)} \right\} \times \left\{ 1 + \frac{AEL^2p}{Rc_p r_s(T_I)} \cdot \frac{r_s(T_I)}{T^2} \right\} \quad (18)$$

where we have also made the assumption that  $r_s(T_I)/T^2 \approx r_s(T_I)/T_I^2$ .

We can similarly obtain

$$\frac{p}{r_s(T)} = \frac{p}{r_s(T_I)} \left\{ 1 + \frac{AEL^2p}{Rc_p r_s(T_I)} \cdot \frac{r_s(T_I)}{T^2} \right\} \quad (19)$$

$$\frac{L}{r_s(T)} = \frac{L}{r_s(T_I)} \left\{ 1 + \frac{AEL^2p}{Rc_p r_s(T_I)} \cdot \frac{r_s(T_I)}{T^2} \right\} \quad (20)$$



The parameterisation of the precipitation process gives values of  $P/r_s(T_I)$  as a function of  $r_I/r_s(T_I)$  so that  $r_I/r_s(T_I)$  can be obtained from (18) for values of the observed relative humidity  $r/r_s(T)$ . Substitution into (19) and (20) enables the precipitation rate and the liquid water content to be calculated. In fig 3 are plotted curves of the variation of  $P/r_s(T)$  with the observed relative humidity for various values of the parameter A and the temperature dependent factor  $B = EL^2 r_s(T_I)/Rc_p T_I^2$ . In the operational forecasts the analysis scheme uses forecast fields following condensation and precipitation as a background field for the relative humidity analysis so that in this case consistency between observations and the model is achieved by setting  $A = 0$ . This has the added advantage of removing the temperature dependent factor from the equations. Having calculated the precipitation from a layer from the initial relative humidity the surface precipitation is readily obtained by integration downwards from the highest level treating evaporation of precipitation in the same way as is used in the forecast model. Since the changes in lower layers resulting from the evaporation of precipitation falling through them are assumed to be treated together with the dynamical changes they do not affect the precipitation from these layers.

Using the method described above the rainfall rates have been deduced from initial relative humidity fields for an occasion in October 1975 the results being shown in fig 4(a). The manual surface analysis and the observations are shown in fig 4(b). It can be seen that in general there is good agreement between the observations of rainfall and the location of the rainfall deduced from the relative humidity analyses. There are some discrepancies particularly over the sea but these can probably be explained by the scarcity of upper level humidity observations in this area and the consequent reliance on the background field, which contains the normal forecast errors, to provide analyses.

##### 5. The effects of the revised parameterisations on 10-level model forecasts

A number of forecasts have been re-run using the revised parameterisation of condensation and precipitation to test the affects both on single forecasts and the cumulative effects which would be obtained in an operational environment. As has



been mentioned, forecast fields are used as background fields in the operational data analysis scheme but it was discovered that the revised parameterisation resulted in forecasts with about 10% lower mean relative humidities than using the operational parameterisation. It was decided therefore that the analyses for the forecasts should be re-run using the revised forecasts as background fields; in these re-analyses bogus humidity data were suppressed as these were based on experience with the operational forecast.

The Rectangle forecast from 00 GMT 12 January 1974 was examined in detail. During the period of this forecast a weak depression centred in mid-Atlantic deepened rapidly as it approached the British Isles and by 00 GMT 12 January the central pressure, according to the initial charts, had decreased from 1003 mb to 962 mb. The two relevant initial surface charts are shown in fig 5. The operational forecast is shown in fig 6 together with a forecast using the revised parameterisation. In both cases the position of the centre is similar and incorrectly forecast but the revised formulation gives 7 mb more development. The extensive area of slight rain in the revised forecast is a defect which can be removed by the use, in conjunction with the revised condensation parameterisation, of a deep convective scheme (Hayes, 1976). This organises the precipitation into areas of convective rain while, in this example, not affecting the surface pressure forecast. In order to assess the usefulness of the revised parameterisation schemes compared with simpler schemes, the operational forecast was re-run with the threshold humidity for condensation reduced to 80%, and all of the condensed water precipitated. It can be argued that since the revised parameterisation allows precipitation from layers where the mean relative humidity is less than 100% some allowance should be made for the evaporation of precipitation within the layer from which it falls as well as in lower layers. The forecast with the revised parameterisation was re-run with this modification. In both of the modified forecasts there were no significant changes in the position of the developing centre but the temporal variation of the depth is shown in fig 7(a).

As has been noted earlier a defect of the current operational forecast in the low rainfall accumulations achieved in the early stages of the forecast, about



6-12 hr for the Rectangle fine mesh forecast, and up to 24 hr for the Octagon forecast. This arises, at least in part, from the low initial relative humidities which seldom exceed 90% even in areas of observed precipitation. It is therefore necessary that time should elapse before the numerical model produces precipitation and this can be observed in successive rainfall rates averaged over the 6 hr period and over the whole forecast area. These are presented in fig 7(b) for the forecasts described above. The operational forecast and that in which there is evaporation of precipitation within the layer of formation, which effectively increases the threshold relative humidity for precipitation from a layer to approaching 100%, both have much smaller rainfall accumulations in the early stages of the forecast than in later periods. In this example the slow decrease in the rainfall rate after 9 hr arises from synoptic effects. In the forecasts with a reduced threshold the defect is less noticeable and that overall accumulation of rainfall are increased.

As a result of this and a limited number of similar experiments it was concluded that the revised parameterisation scheme would provide better forecasts of rainfall accumulations and improved development. Subsequent tests were therefore limited to tests over an extended period in both Rectangle and Octagon versions of the forecast of the parameterisation scheme described in this note.

A sequence of ten forecasts covering the period 00 GMT 4 March 1976 to 12 GMT on 8 March 1976 were re-run using the revised parameterisation. New analyses were carried out using as background fields the 12 hr forecasts obtained with the experimental parameterisation. Some examples of the Rectangle 24 hr forecasts are shown in fig 8 where they are compared both the operational forecast and with the verifying operational initialisation. The initialised surface charts for the experimental forecast are also shown and in those examples where there is overlap between a verifying initialisation and a subsequent experimental initialisation the very small differences can be seen. The experimental initialised charts are shown with an initial rainfall rate derived in the way described earlier.

In the forecasts from 00 GMT on 4 March, see fig 8(a), the deepening and movement of a small depression in the Atlantic were almost identically treated by both forecasts,



both failed to deepen the depression sufficiently or to move it sufficiently rapidly. However in the experimental forecast the leading edge of the rainbelt was more advanced and rain was observed in Western parts of the British Isles by 00 GMT on 5th. There are no significant differences between the two surface pressure forecasts but the more extensive rainfall predicted by the experimental forecast over Eastern Europe is more in agreement with the observations. The moderate rain forecast to the West of Italy and which was enhanced by the revised parameterisation scheme was not observed.

The forecast from 12 GMT 4 March was much better than the preceeding forecast and is shown in fig 8(b). Although both forecasts underestimate the deepening of the Atlantic depression the position is quite well forecast. In this example the central pressure after 24 hr is about 3 mb deeper with the revised parameterisation scheme than with the operational forecast. The rather more extensive areas of rain over the Adriatic and Eastern Europe on the forecast using the revised parameterisation are more in agreement with the observations than the distributions from the operational forecast.

Fig 8(c) shows the rather poor forecasts produced from the 00 GMT date on 5 March. Both forecasts failed to predict the development in this period. There are only small differences between the two surface pressure forecasts and minor differences in the distribution of the rainfall. This was the only forecast in which the mean 36 hr rainfall accumulations with the revised parameterisation were less (by about 2%) than those obtained with the operational model. In contrast to these poor forecasts the forecasts from 12 GMT on 6 March shown in fig 8(d) were quite good. Both versions of the forecast correctly brought the depression in across the western boundary of the model although by 24 hr the revised version of the forecast had a central pressure some 2 mb deeper than the operational version and more in agreement with the observations. The treatment of the depression moving towards Spain was also very similar in both models although again the central pressure was slightly lower in the revised forecast.



Small pressure differences are the major differences between the forecasts from 00 GMT 8 March. The depression to the west of Greenland is some 3 mb deeper in the revised forecast although the central pressure is still about 7 mb higher than was observed. It is also interesting that the revised formulation has given rise to a much sharper defined frontal rainbelt approaching the British Isles than was predicted by the operational formulation. Observations showed that both forecasts predicted too much rain on this front. Over Europe both versions of the forecast appear similar.

From the results of these forecasts it can be seen that the affect of the revised parameterisation on the synoptic forecasts is small. There are differences of a few millibars in the central pressure of developing depressions and most of these changes are improvements. There is also some indication that the positioning and sharpness of the rainbelts is improved by this formulation. The major effect of the parameterisation on the rectangle forecast is in the mean rainfall rates. In fig 9(a) the successive 6 hr accumulations of rainfall over the inner part of the forecast area are expressed as fractions of the 36 hr accumulation; the results being the mean values over the 10 forecasts. It can be seen that the accumulation in the first 6 hr is increased by almost 50% with the revised parameterisation and that there is only a 10% variation in the accumulation throughout the forecast; and affect of the parameterisation is therefore to reduce one of the noted defects of the present rainfall forecasts. It was noted that in general the revised parameterisation results in greater rainfall accumulations than the operational parameterisation and the ratio of the 36 hr accumulations are shown for each of the sequence of 10 forecasts. The average increase is about 7% with the revised parameterisation but there is considerable scatter about this figure and, as has been noted, one of the revised rainfall forecasts was lower than the operational version; this was associated with a very poor synoptic forecast from both the revised and operational versions of the forecast.

In these assessments of the effects of the revised parameterisation of the condensation and precipitation processes on 10-level model forecasts attention has been concentrated on the effects on the fine mesh forecasts since these are used to



derive precipitation forecasts and it has been shown that the synoptic effects are small. However as has been noted the parameterisation was incorporated into the coarse mesh version of the model since the latter is used to provide the background fields, and therefore the data over much of the rectangle forecast area. An examination of the coarse mesh forecasts showed that the synoptic changes resulting from the revised parameterisation were very small and in general where there was a change in the fine mesh forecast, the change in the coarse mesh forecast in the same area was about half of that in the fine mesh forecast at 24 hr and rather less than this later in the forecast. An improvement was noted in the statistical behaviour of the rainfall forecasts, the accumulation during the first 12 hr of the forecast being increased by about 25% relative to the accumulations later in the forecast although they were still lower than those for the later periods.

## 6. Conclusions

The parameterisation of the condensation and precipitation processes which has been described in this note has been an attempt to take account of latent heating within some fraction of the volume represented by a grid point when the mean relative humidity is less than 100%. The conversion from cloud water to precipitation has been dissociated from the latent heat release with the possibility of evaporation of cloud water in the regions behind frontal rainbelts. A steady state approximation enables rainfall to be diagnosed from relative humidity data and the results are in reasonable agreement with observations.

When the parameterisation is included in 10-level model forecasts the additional release of latent heat can give rise to small changes in the surface pressure forecast particularly in the vicinity of rapidly developing systems. Improvements or changes in the positioning of centres are not obtained and this is in common with experience at the present time which suggests that significant improvements in the synoptic behaviour of the 10-level model forecasts are not to be found by the improvement of the parameterisations of the physical processes. There are however considerable improvements in the statistical behaviour of the rainfall forecasts. There is an overall increase of between 5 and 10% in the rainfall accumulations and



the rainfall in the initial stages of the forecast is comparable with that in later stages. There is some indication that the shape of the rainbelts is improved by the revised parameterisation and this can result in considerable improvements in the forecasting of the timing of the onset of precipitation.

In operational use the revised parameterisation would have two disadvantages; it requires about 10% more computing time for a forecast with the revised parameterisation than one with the operational parameterisation because the routine which calculates the latent heating is required at all grid points and not just at those where the air is saturated. Also the use of liquid water as a model variable at 7 levels requires more storage in the forecast data sets. Against this is the small improvement in the synoptic behaviour of the rainfall and surface pressure forecast and the considerable improvement in the early rainfall rates which could be useful if the 10-level model was used to produce short period rainfall forecasts. The diagnosed rainfall rates from the relative humidity data would be of use to those involved with the use of subjective humidity data for modifying the initial relative humidity fields and the incorporation onto the initialised surface pressure charts of derived rainfall may add credibility to these charts.



# References

- |                              |      |   |
|------------------------------|------|---|
| Atkins, M J                  | 1970 | Objective analysis of upper air height and humidity data on a fine mesh, Met Mag, 99, pp 98-110.                          |
|                              | 1974 | The objective analysis of relative humidity, Tellus, 26, pp 663-671.  |
| Benwell, G R R               | 1971 | The Bushby-Timpson 10-level model on a fine mesh. Meteorological Office Scientific Paper 32., HMSO, London.               |
| Gadd, A J; Keers, J F;       |      |   |
| Timpson, M S and White, P W  |      |   |
| Bushby, F H and Timpson, M S | 1967 | A 10-level atmospheric model and frontal rain. Quart Jnl Roy Met Soc, 93, pp 1-17.  |
| Hayes, F R                   | 1976 | A new parameterisation scheme of temperate latitude convection in the 10-level model. Submitted to Quart Jnl Roy Met Soc. |
| Jonas, P R                   | 1976 | The use of surface synoptic data to estimate upper-level relative humidity over the sea. Met Mag, 105, pp 44-56.          |
| Mason, B J                   | 1971 | The Physics of Clouds, 2nd Edition. Oxford University Press.  |
| Wickham, P G                 | 1974 | Some examples of rainfall forecasts produced by the fine mesh version of the 10-level model. Met Mag, 103, pp 209-224.    |



## List of Figures

- Fig 1 The variation with mean total relative humidity of (a) the liquid water mixing ratio averaged over the volume and (b) the average liquid water mixing ratio in the cloud. Normal distributions of total relative humidity are assumed with the indicated standard deviation  $\sigma$ . For the unlabeled curve  $\sigma$  decreases linearly from 0.4 for a mean humidity of 0% to 0.2 for a mean humidity of 100%.
- Fig 2 The distribution of humidity observations at 850 mb. The solid line shows the total distribution and the dotted line shows the distribution for occasions defined as wet. The broken line shows the distribution expected on wet occasions using the parameterisation scheme and the observed total distribution.
- Fig 3 The variation of derived precipitation rate with observed relative humidity. The liquid water precipitation has been converted to a rainfall rate assuming constant precipitation from a 100 mb deep layer over a 12 min period. Curves are plotted for different values of the parameter A and for different values of the temperature dependent factor  $B = \epsilon L^2 r_s(T_E) / R c_p T_E^2$ .
- Fig 4 The surface analysis for 12 GMT 14 October 1975. (a) The numerical surface pressure analysis and rates of rainfall derived from numerically analysed humidity fields. The symbols +,  $\diamond$  and  $\star$  denote rainfall rates in the ranges 0.1-0.5, 0.5-4.0 and greater than 4.0 mm hr<sup>-1</sup> respectively. (b) The Central Forecast Office hand analysis and the observations for the same time and for the same area as (a).
- Fig 5 The surface analyses for (a) 00 GMT 11 January 1974 and (b) 00 GMT 12 January 1974.
- Fig 6 Forecast surface charts showing the rate of precipitation verifying at 00 GMT 12 January 1974. The 24 hr forecasts were produced using (a) the operational and (b) the revised parameterisation of condensation and precipitation.
- Fig 7 The variation throughout the forecasts from 00 GMT 11 January 1974 of (a) the central pressure of the developing mid-Atlantic depression and (b) the 6 hr

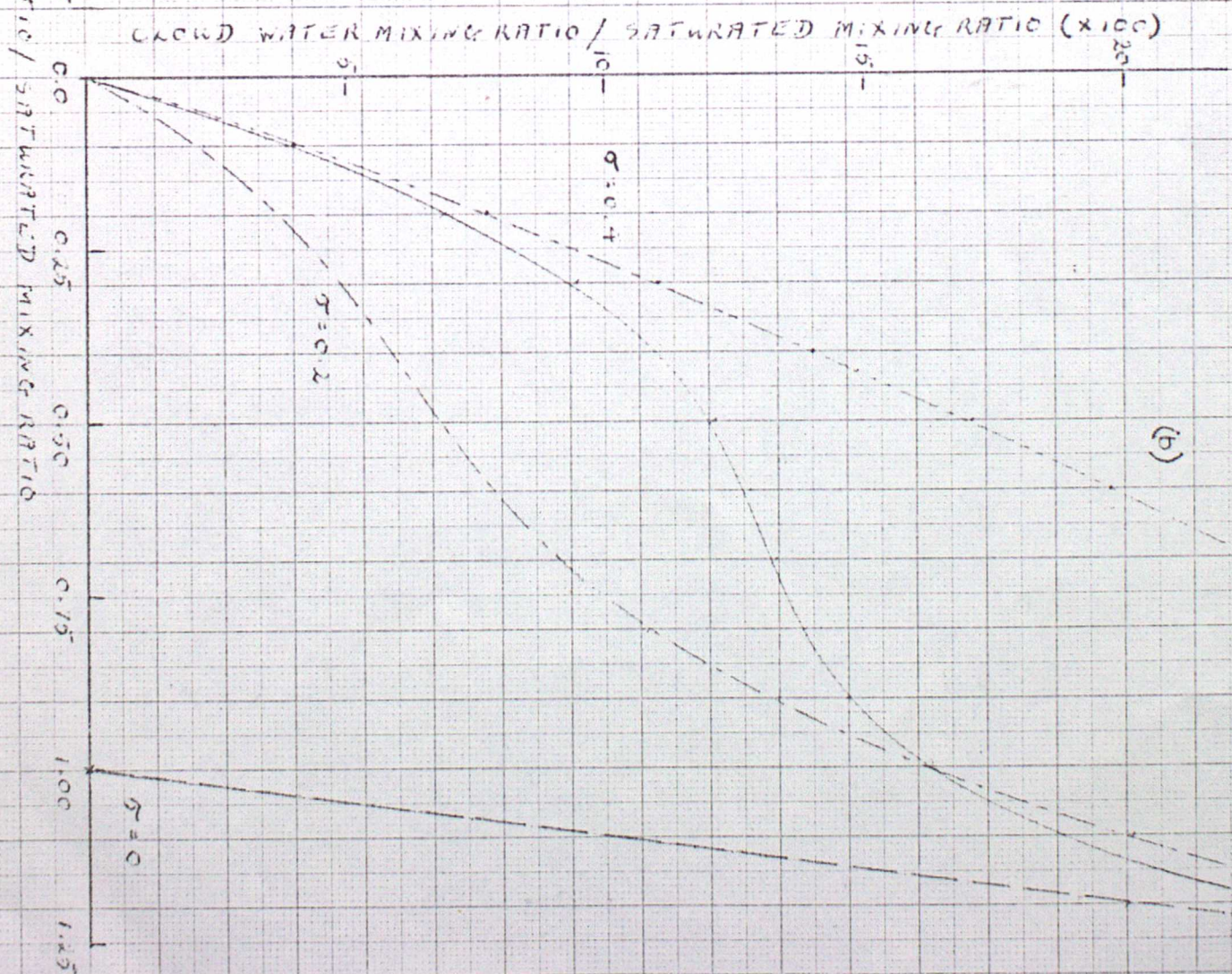
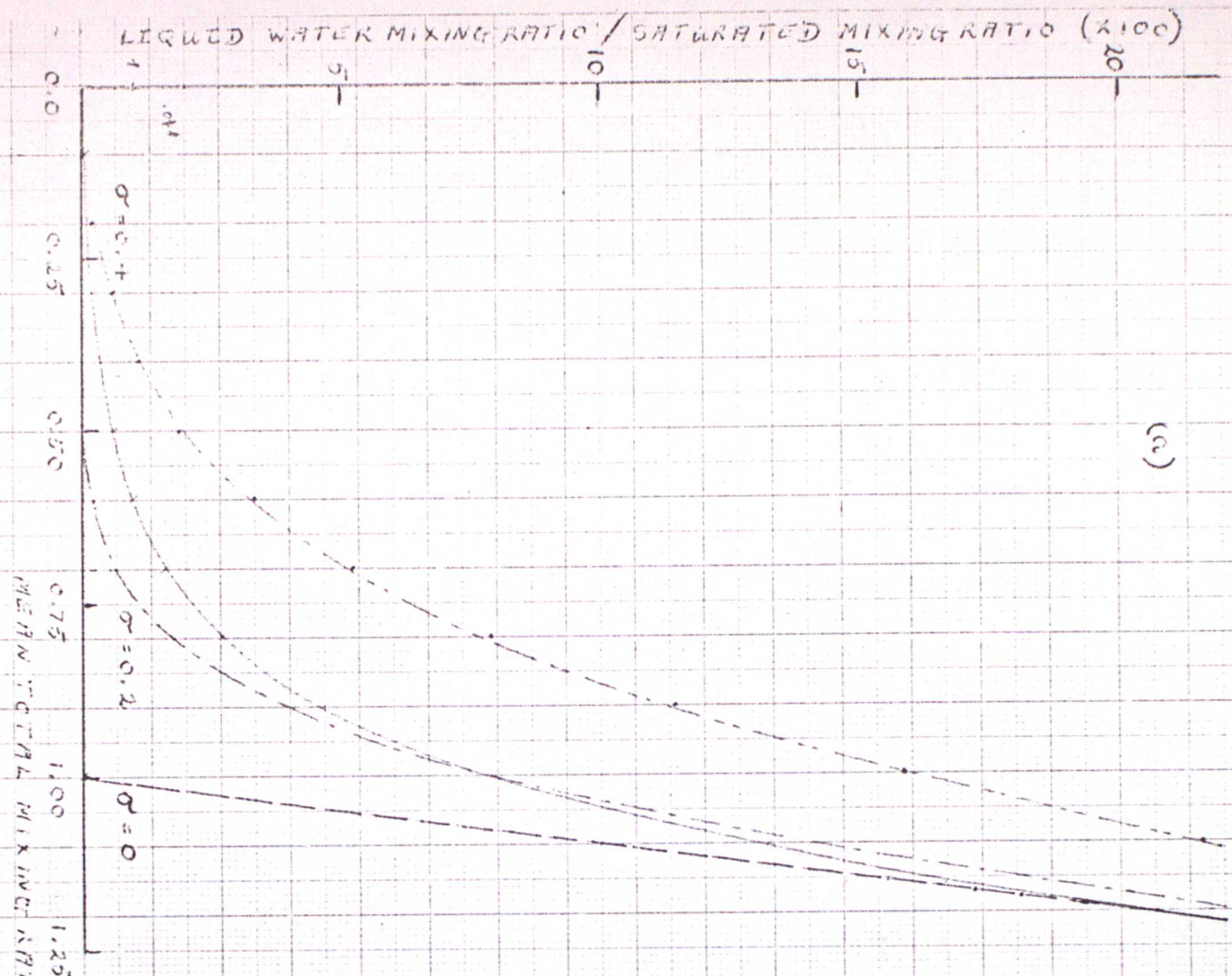


average rainfall rate. The forecasts are I, operational; II, operational with threshold reduced to 80%; III, revised; IV, revised with evaporation of precipitation in the layer of formation.

Fig 8 Charts of surface pressure and instantaneous rainfall rate from initialisation and 24 hr forecasts using the operational and experimental parameterisation of condensation and precipitation. For each forecast the experimental initialisation and the verifying operational initialisation are shown together with the two 24 hr forecasts. Some idea of the small differences between the two initialisations can be seen where successive forecasts overlap, eg (a) and (b).

Fig 9 The effects of the revised parameterisation on the average rainfall accumulation for the rectangle forecasts area. (a) The ratio of successive 6 hr accumulations, averaged over 10 forecasts, to the 36 hr accumulation. The solid line shows the results for the revised forecasts and the dashed line shows the operational results. (b) The ratio of the revised 36 hr accumulation to that from the operational forecasts for each of 10 successive forecasts. The mean ratio is 1.07.







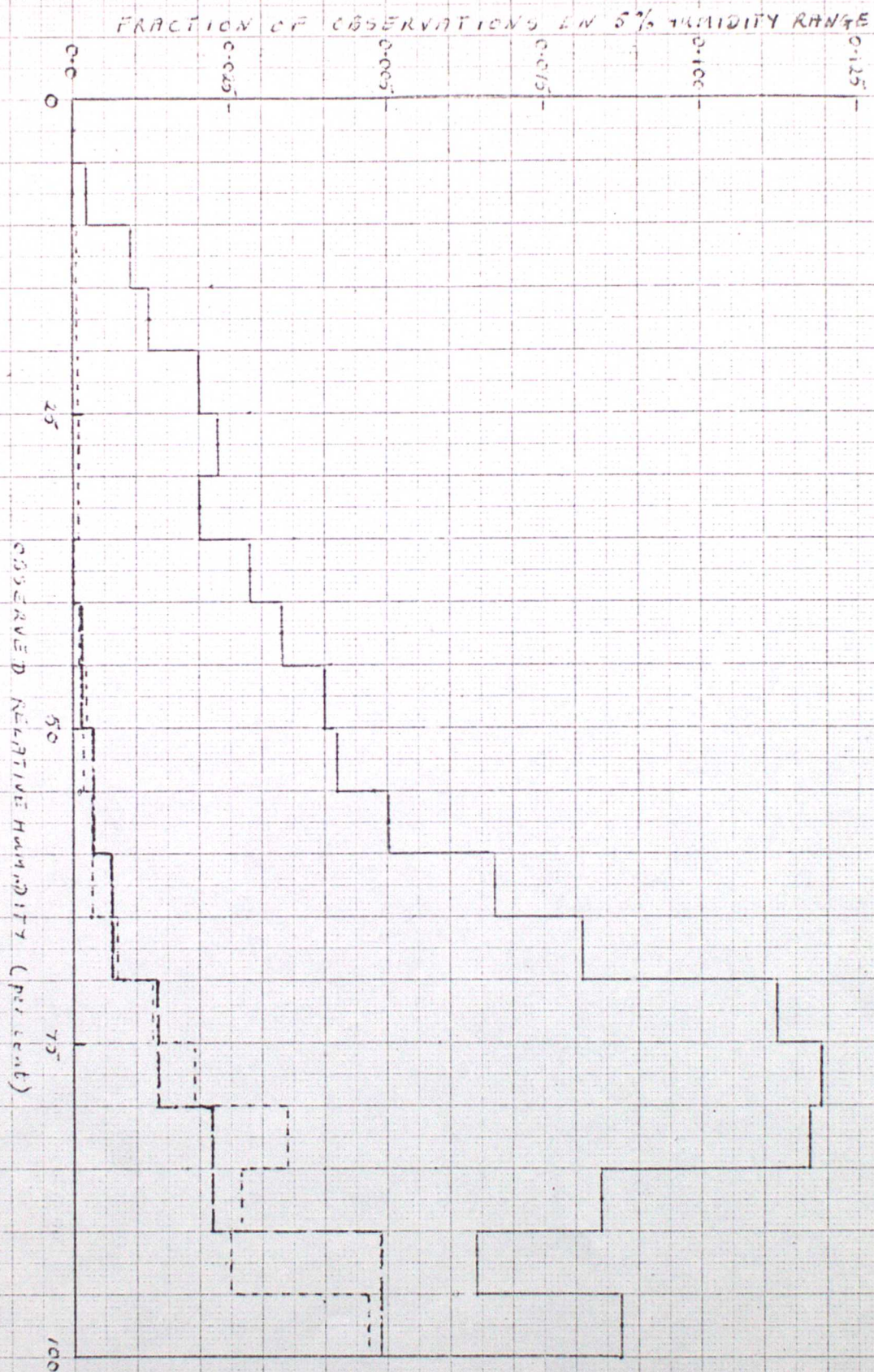




Fig 3

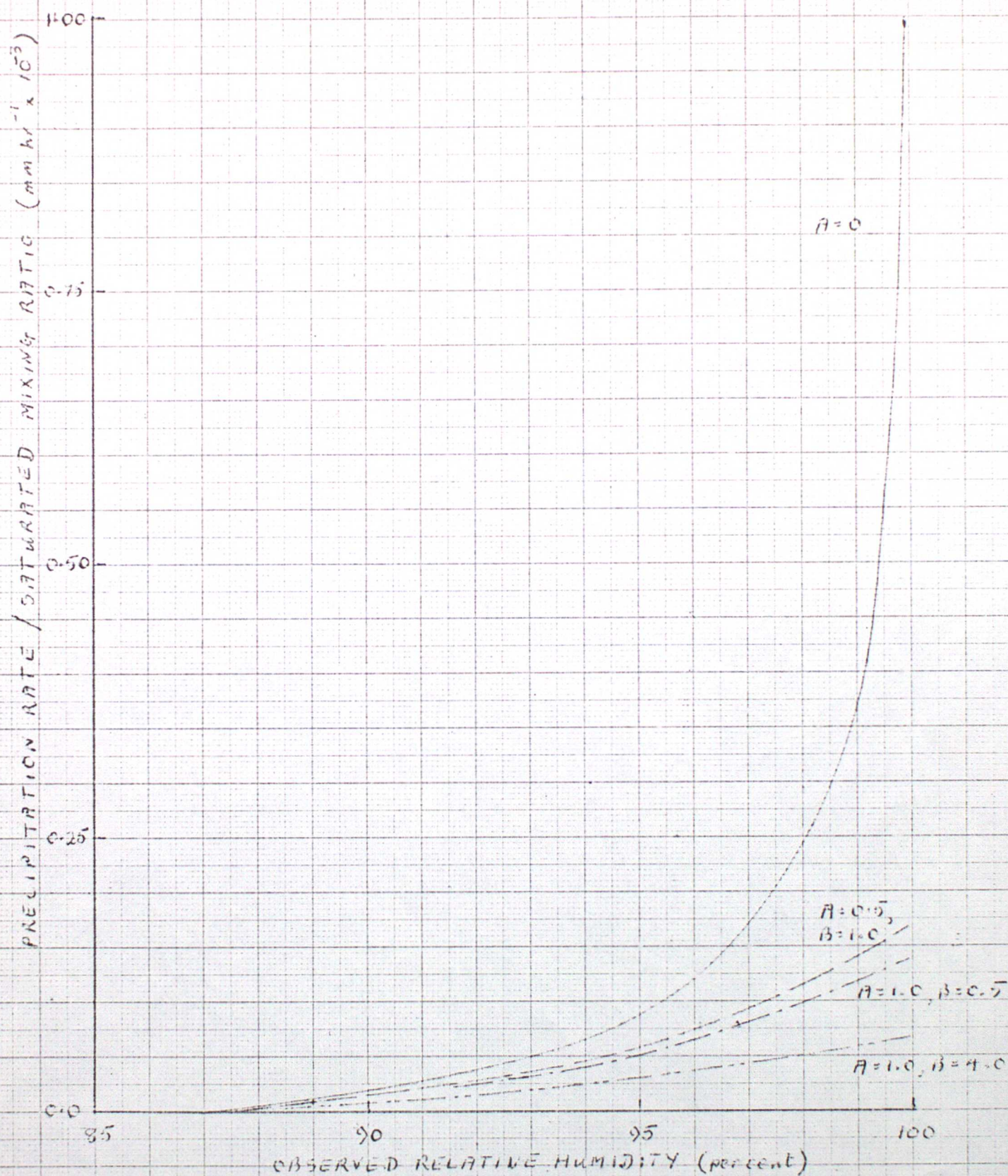




Fig 4 (a)

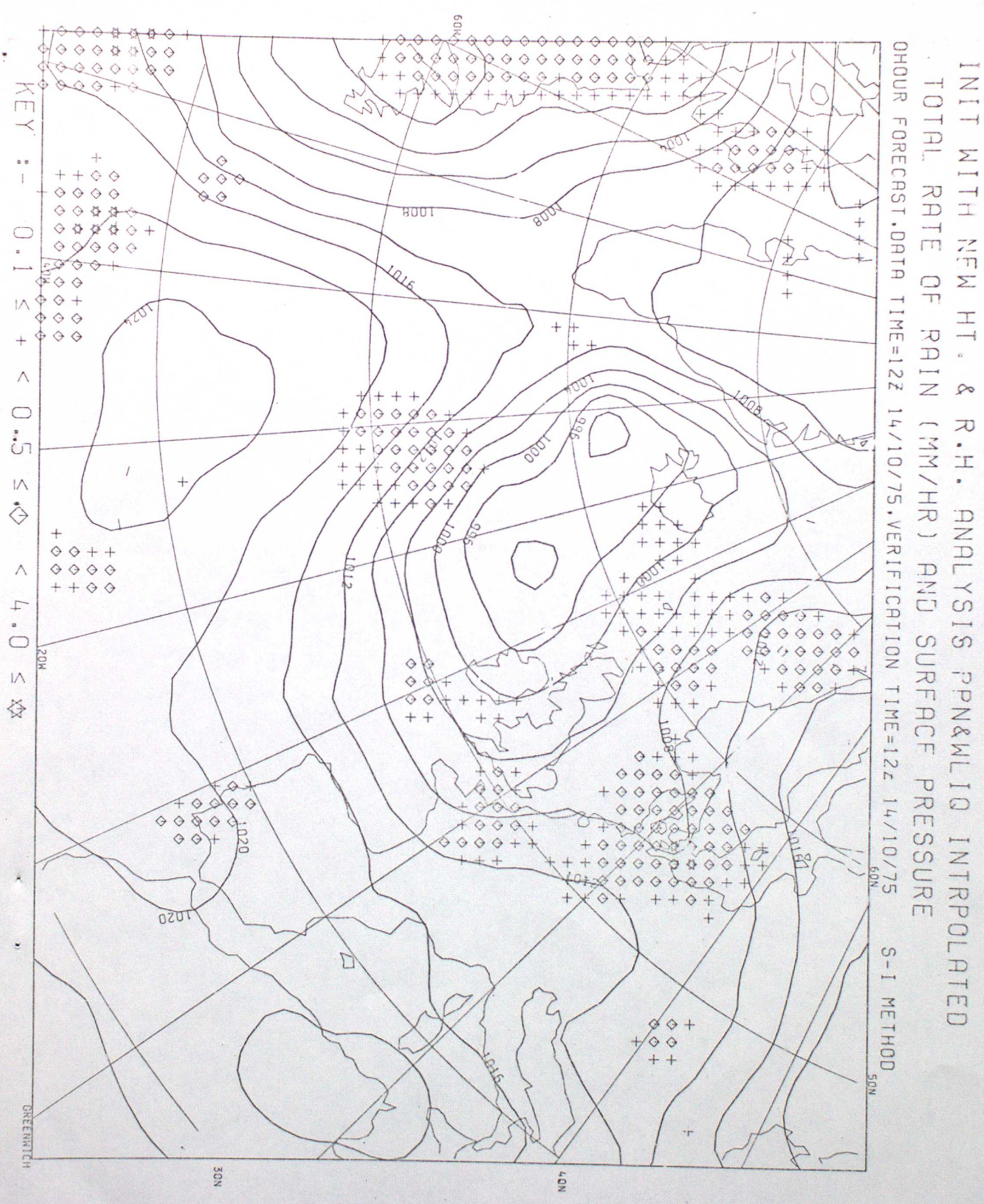






Fig 4 (b)



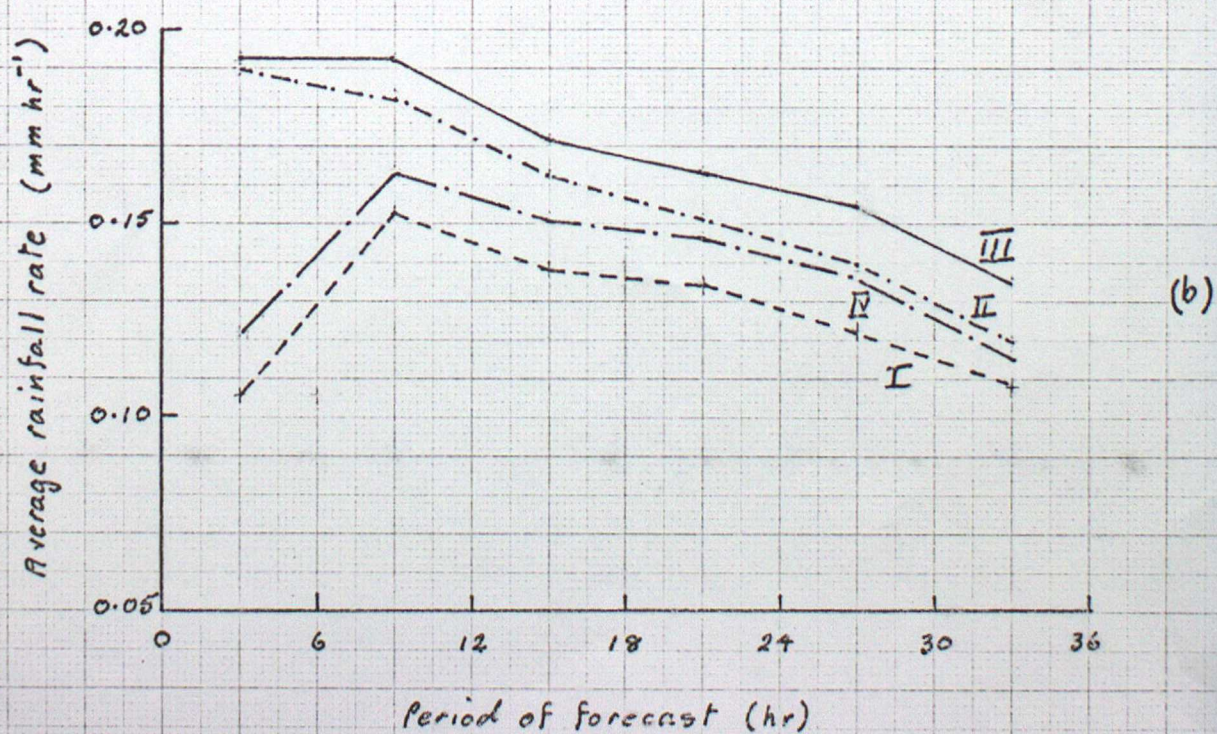
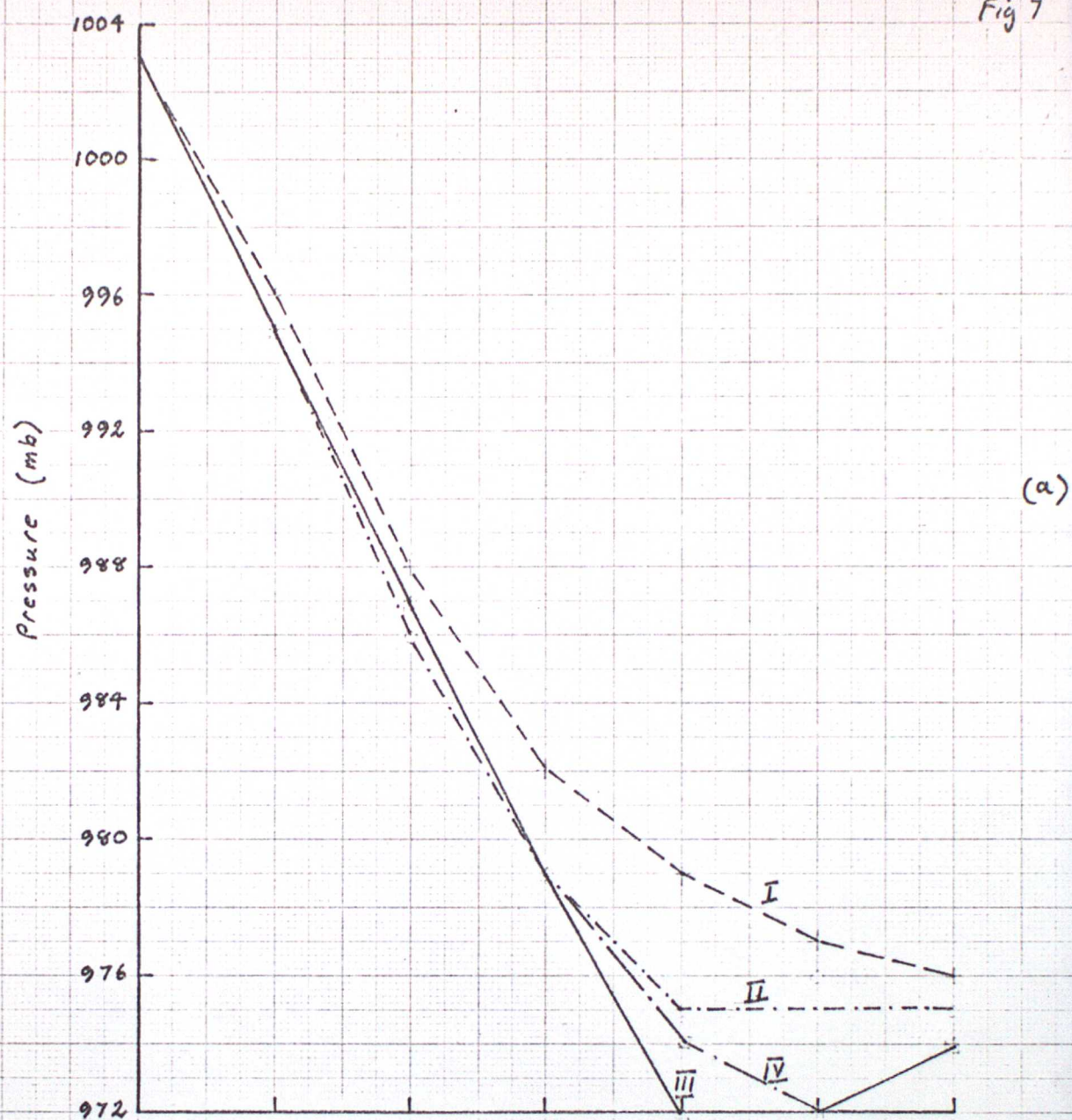




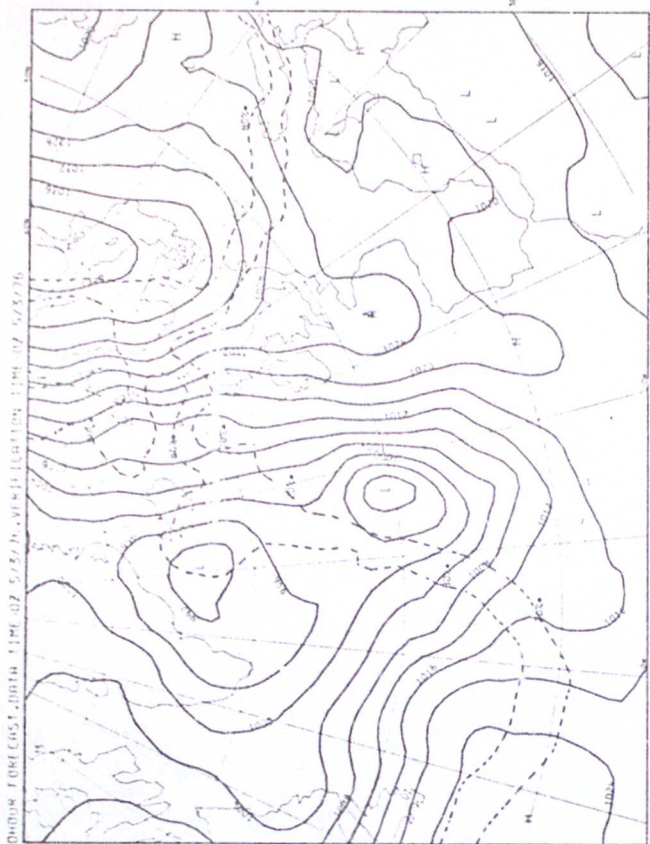




Fig 7

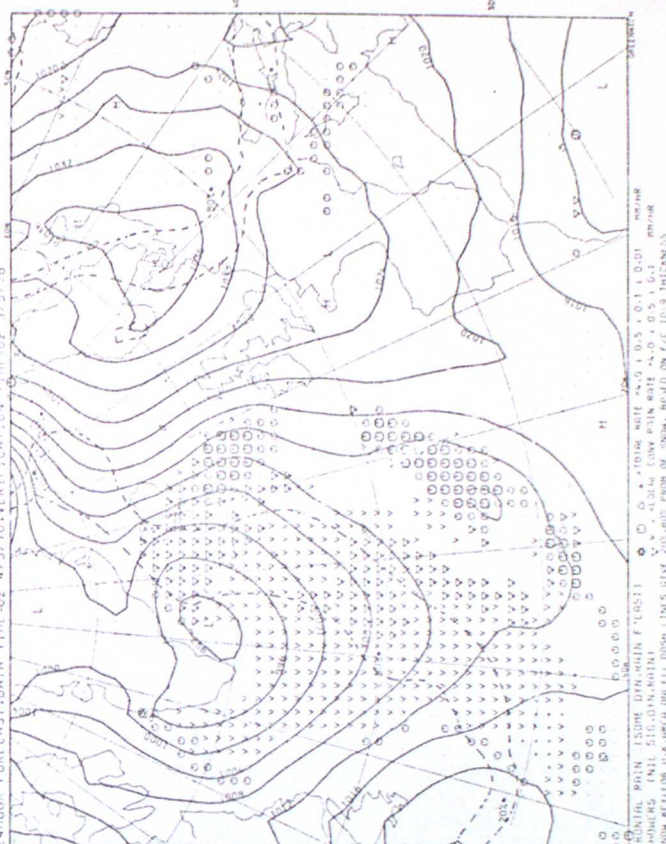






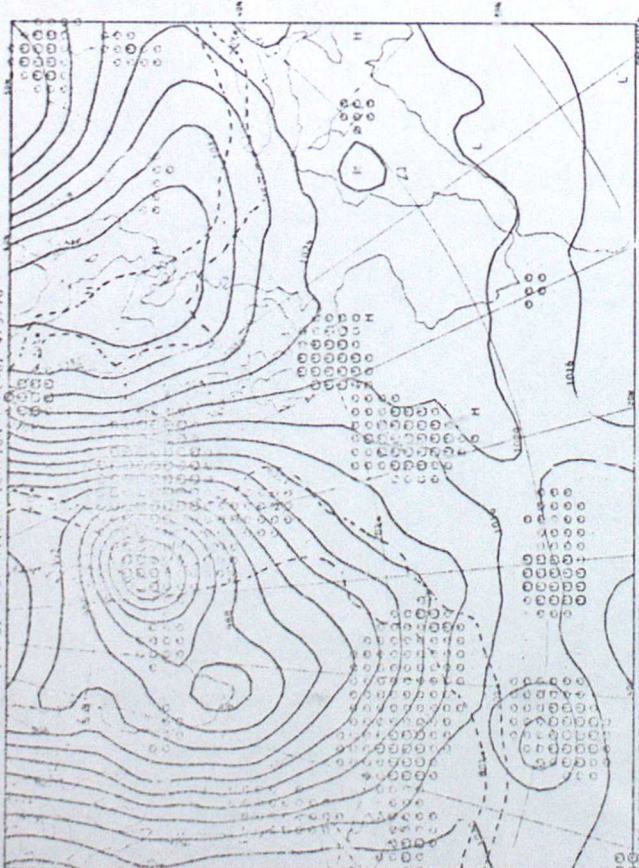
RUNTAL RAIN ISOME DYN. RAIN F. CAST)       $\odot$   $\odot$   $\odot$  TOTAL RAIN  $\pm 0.0 \pm 0.5 \pm 0.1 \pm 0.01$  MM/HR  
 PROWMS (NII SIG-DYN. RAIN)       $\nabla$   $\nabla$   $\nabla$  TOTAL CUM. RAIN RATE  $\pm 0.0 \pm 0.5 \pm 0.1$  MM/HR  
 HOW MEIROM U.K. RAIN DNETY DASH LINES GIVE 202-BUS PROB. OF SNOW. BASED ON FVC 10-9 HOURS

## EXPERIMENTAL FORECAST

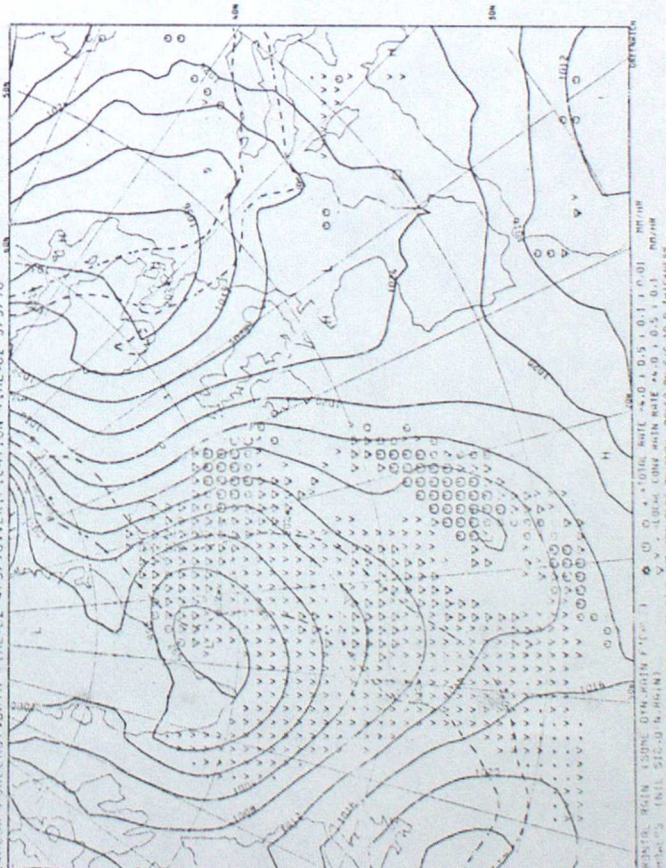
FORECAST SURFACE PRESSURE AND PRECIPITATION  
2-HOUR FORECAST DATA TIME-02 4/3/76-VERIFICATION TIME-02 5/3/76

## EXPERIMENTAL INITIALISATION

Downloaded from ascelibrary.org by University of California, San Diego on 06/25/16. See COPYRIGHT ASCE LIBRARY

[illegible]

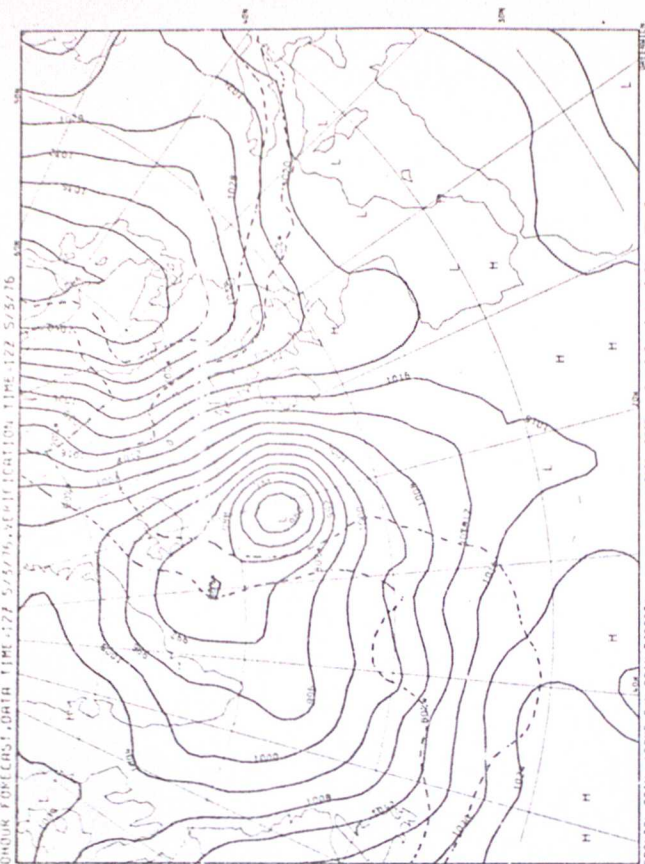
## OPERATIONAL FORECAST

FORECAST SURFACE PRESSURE AND PRECIPITATION  
1-HOUR FORECAST DATA TIME-02 4/3/76-VERIFICATION TIME-02 5/3/76



# VERIFYING OPERATIONAL INITIALISATION FORECAST SURFACE PRESSURE AND PRECIPITATION

CONCUR FORECAST, DATA TIME: 17 5/3/76, VERIFICATION TIME: 122 5/3/76

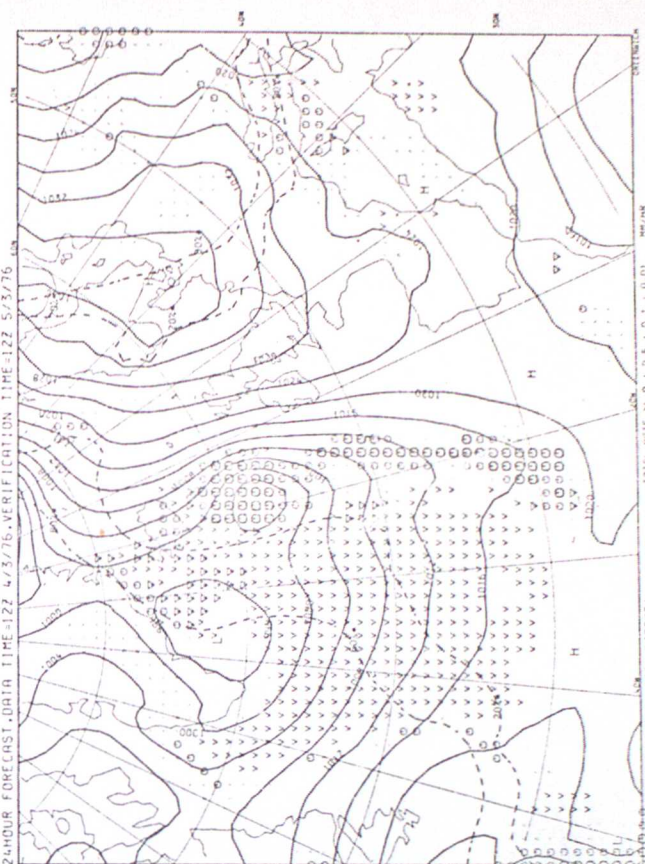


RENTAL RAIN ISOPE DYN. RAIN F-CAST)  $\Phi$   $\Phi$   $\Phi$  \* TOTAL RATE  $\times 0.1$   $0.5$   $1.0$   $1.0$   $0.01$  MM/HR  
 SNOWERS INIL SIG-DYN. RAIN)  $\Psi$   $\Psi$   $\Psi$  \* LOCAL CNV RAIN RATE  $\times 0.1$   $0.5$   $1.0$   $1.0$   $0.1$  MM/HR  
 SNOW RETION U.S. AREA ONLY: CASH LINES GIVE 203.80% PROB OF SNOW. BASED ON F/C 10-9 THICKNESS

## EXPERIMENTAL FORECAST

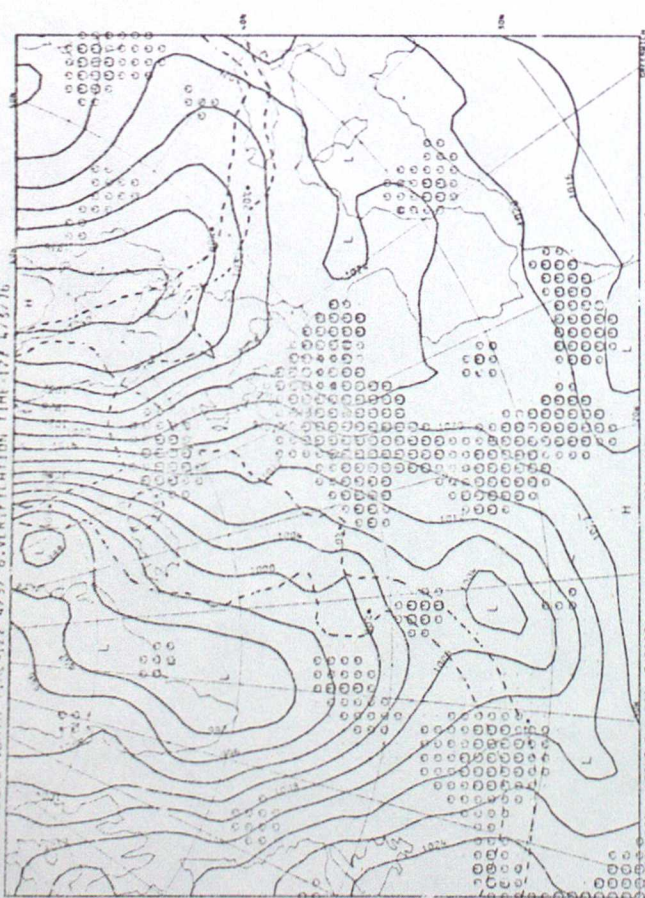
FORECAST SURFACE PRESSURE AND PRECIPITATION

24 HOUR FORECAST, DATA TIME=122 4/3/76, VERIFICATION TIME=122 5/3/76

[illegible]

EXPERIMENTAL INITIALISATION >  
FORECAST SURFACE PRESSURE AND PRECIPITATION

DATE	TIME	WIND	TEMP	PRESS	HUMID	SEA	SKY	REMARKS
04-09	FORECAST							
04-09	12Z	4/5/76	VERIFICATION TIME	12Z	4/8/76			

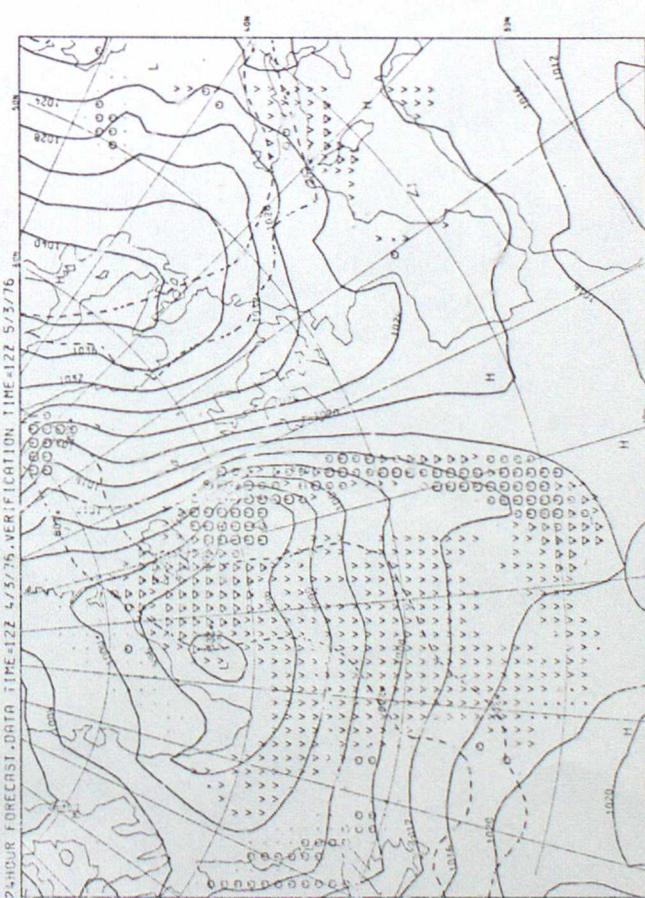


	MM/HR	01
POTENTIAL RAIN (SCHE DYN. RAIN F'CAST)	$\phi \circ \phi$	*TOTAL RATE 4.0 I 0.5 I 0.1 I
SNOWS (NIL SIG. DYN. RAIN)	$\psi \vee$	*LOCAL CONV. RAIN RATE 4.0 I 0.5 I 0
DESIGN PLOT FOR U.S. AREA ONLY: DASH LINES GIVE 20% BOZ PROB OF SNOW. BASED ON F/C 10-9 IMI		*YES

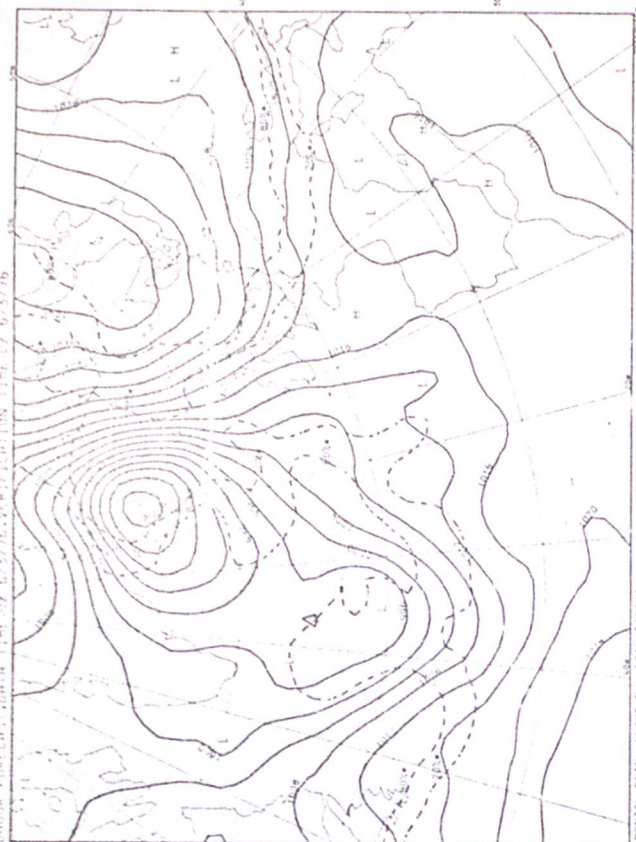
## OPERATIONAL FORECAST

OPERATIONAL FORECAST  
FORECAST SURFACE PRESSURE AND PRECIPITATION

24-HOUR FORECAST DATA TIME=12Z 4/3/76. VERIFICATION TIME=12Z 5/3/76.

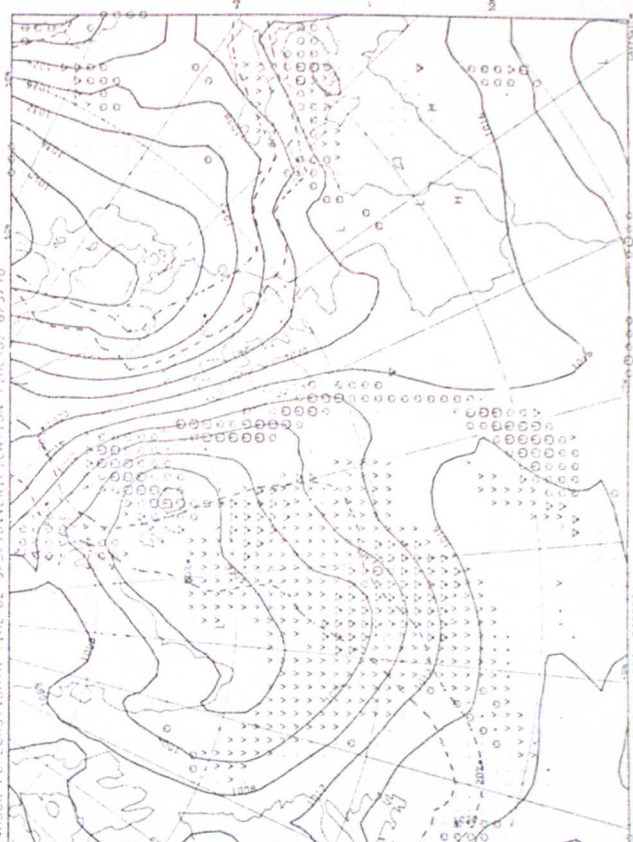
[illegible]





	MONTHLY RAIN	VOLUME DYN. RAIN F(FAST)	$\phi = Q \cdot \text{TOTAL RATE}$	$\pm 0.5 : 0.1 : 0.01$	MM/HR
HOURS IN SL. DYN. PHIN			$\Delta V = \text{VOLUME DYN. RAIN RATE}$	$> 4.0 : 0.5 : 0.1$	MM/HR
HOW MANY U.S. GALLONS PER DAY DASH LINE'S GIVE				FOR 24 HRS. OF SNOW, BASED ON P.F.C. TO 9 HOURS	

## EXPERIMENTAL FORECAST

FORECAST SURFACE PRESSURE AND PRECIPITATION  
 1-HOUR FORECAST DATA TIME 02 5/3/76, VERIFICATION TIME 02 6/3/76

(1)  $\sigma = 10\%$  RATE  $\Delta \sigma = 0.5 \pm 1.1 \pm 0.01$  MEV/K  
 (2)  $\sigma = 1\%$  RATE  $\Delta \sigma = 0.5 \pm 0.5 \pm 0.1$  MEV/K  
 (3)  $\sigma = 0.1\%$  RATE  $\Delta \sigma = 0.5 \pm 0.5 \pm 0.1$  MEV/K

## EXPERIMENTAL INITIALISATION FORECAST SURFACE PRESSURE AND PRECIPITATION

COVER FOR COST, BOTH TIME AND 5/3/76, VERIFICATION TIME OF 5/3/76

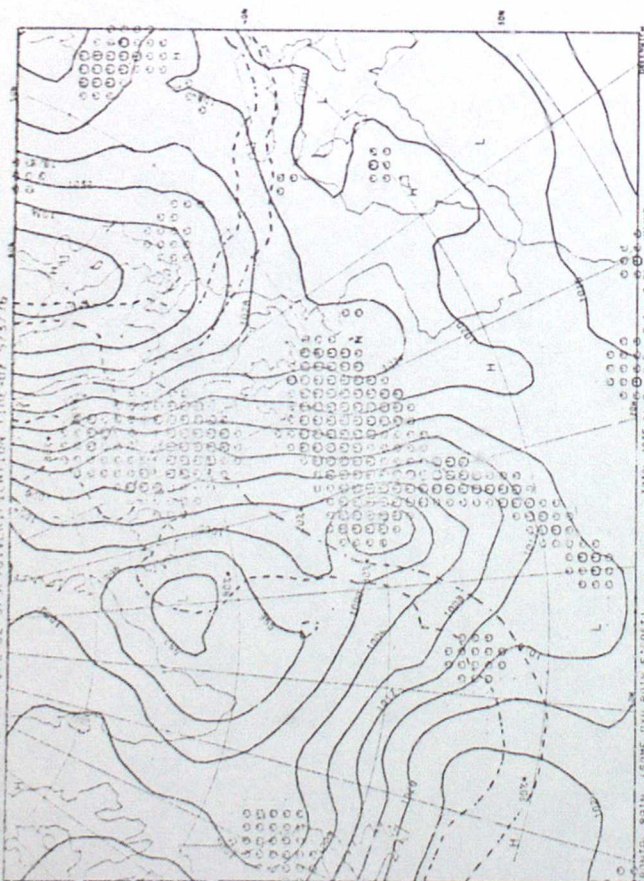
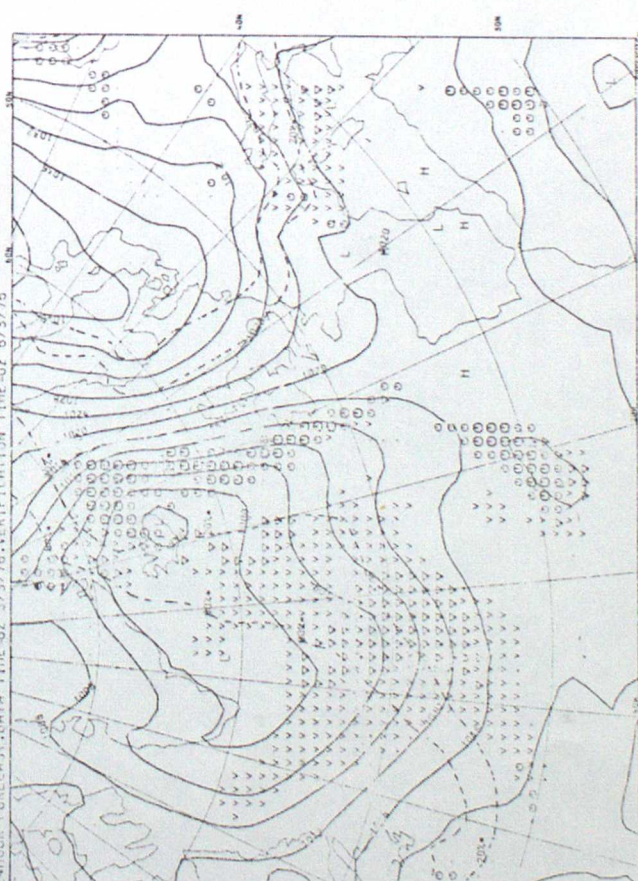
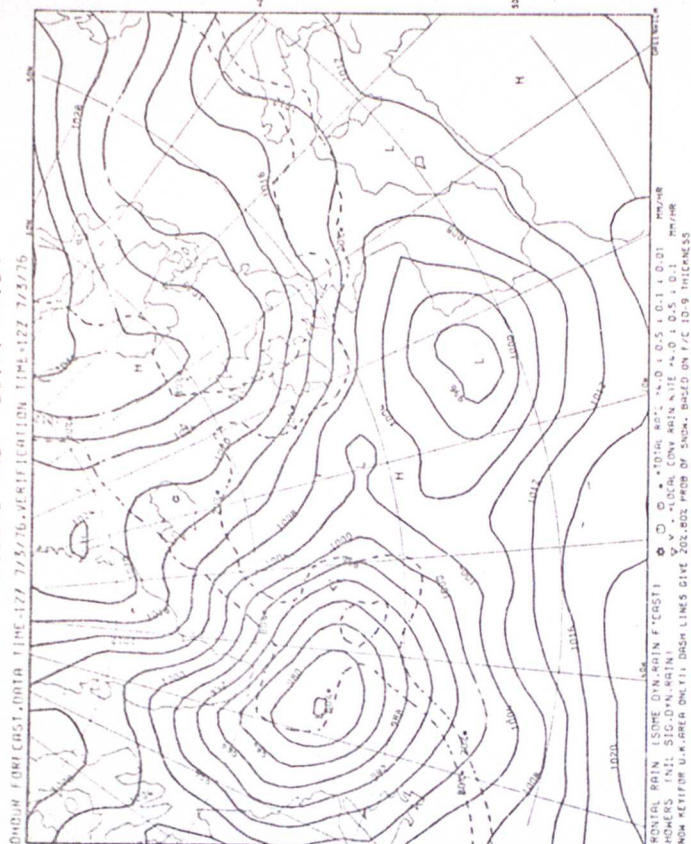


PHOTO. RAIN (SUME DYE. RAIN F. COST)  
 WEATHERS (NIL SIG. DYE. RAIN)  
 204 ACTIFOR V. PAPER ANALYSIS: DASH LINES GIVE 20% MOISTURE OF SW. H. BASED ON F.W. 10-9 THICKNESS

## OPERATIONAL FORECAST

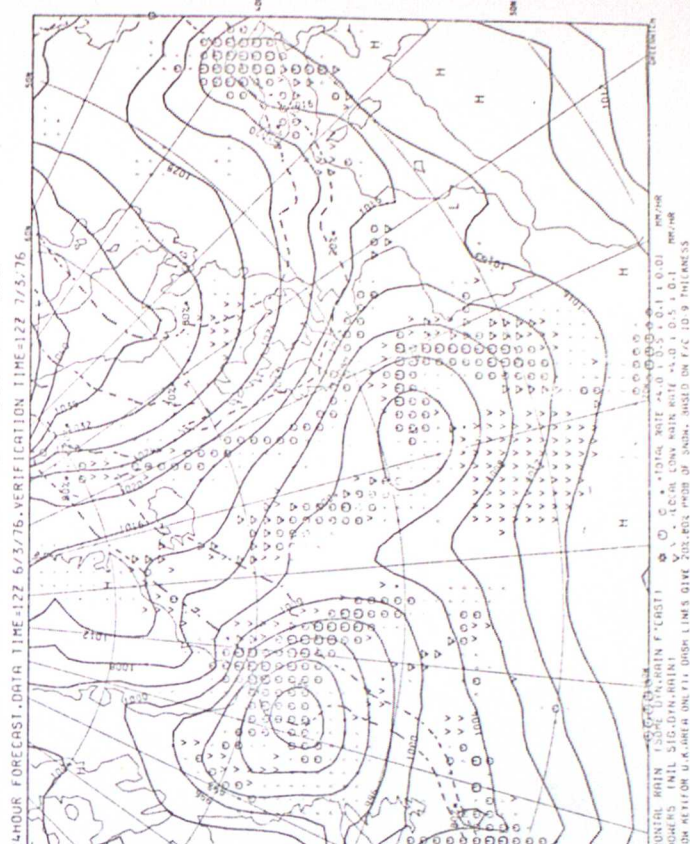
FORECAST SURFACE PRESSURE AND PRECIPITATION  
1-HOUR FORECAST DATA TIME-02 5/3/76, VERIFICATION TIME-02 6/3/76[illegible]





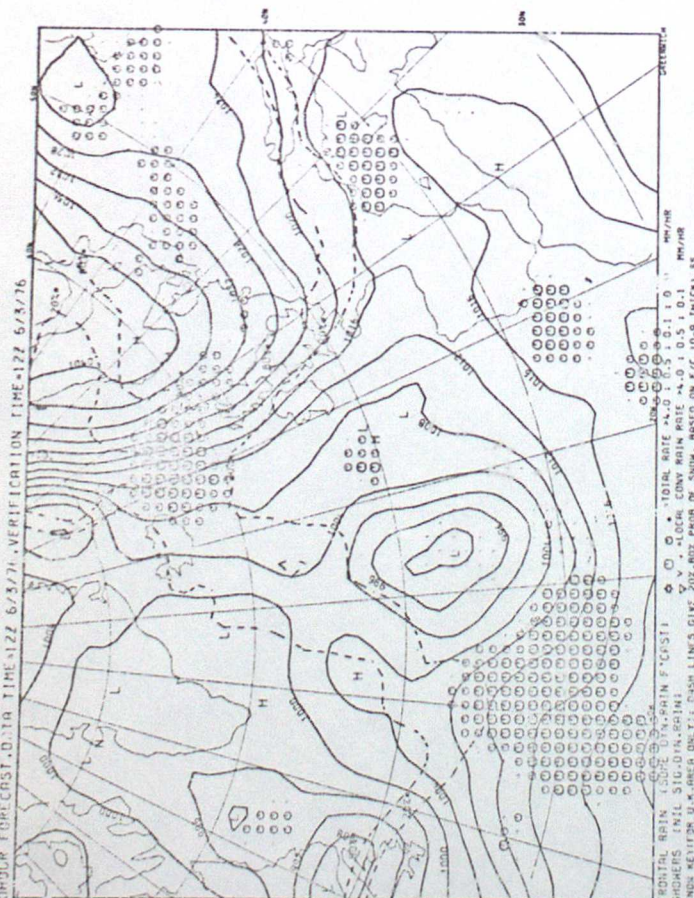
## EXPERIMENTAL FORECAST

FORECAST SURFACE PRESSURE AND PRECIPITATION



## EXPERIMENTAL INITIALISATION

FURCHAST SURFACE PRESSURE AND PRECIPITATION



## OPERATIONAL FORECAST

FORECAST SURFACE PRESSURE AND PRECIPITATION

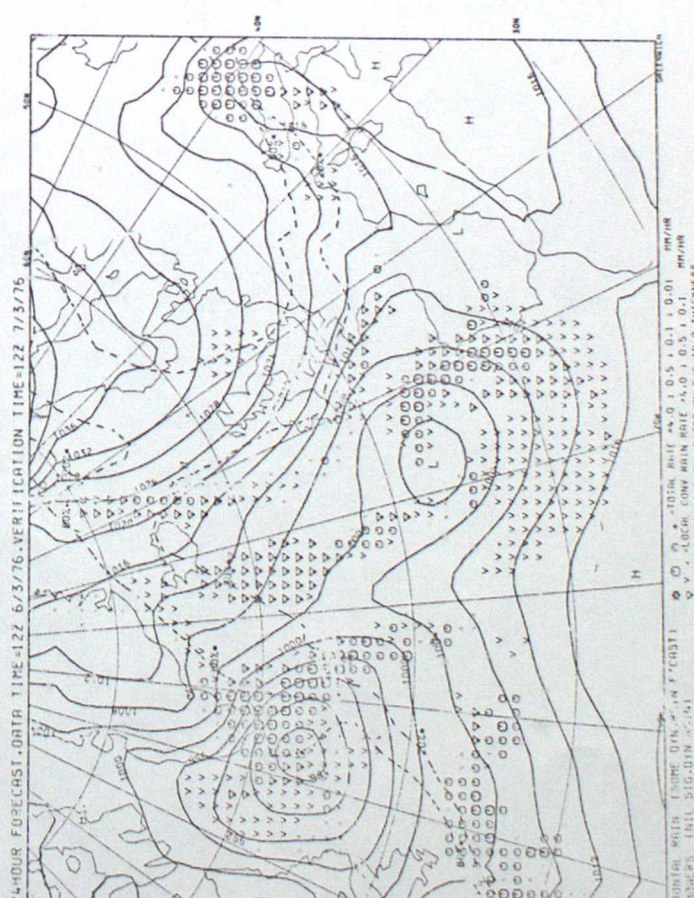








Fig 9

